BASS EXTENSION OF MICROSPEAKER SYSTEM ON MOBILE DEVICE

J. R. Chang* **C. N. Wang**

Department of Engineering Science and Ocean Engineering
National Taiwan University
Taipei, Taiwan

ABSTRACT

This study provides a solution for the bass extension of a microspeaker system in a mobile device that involves using a resonant combination of a front chamber and a rectangular, long, pipe-shaped port. The efficient resonant coupling of the microspeaker system to the acoustic load in this structure enables a microspeaker with modest cone displacement to achieve a high sound pressure level (SPL) and bass extension below the resonance of the microspeaker in free air, and the total dimensions of the structure are minimized. A combination of electro-mechanic-acoustic and finite element methods was applied to determine the SPL and bass extension levels for mobile devices. Simulation results show acceptable agreement with experimental results. A suitable extended-range microspeaker system was applied in a 10 inch tablet. The audio frequency response could be extended from 630 to 300 Hz with the greatest loudness. As much as possible add low bound frequency extension to make the article more clear. Finally, five cases of parameter settings for the front chamber volume, rear chamber volume, rectangular pipe-shaped port, cross-sectional area, and opening area were studied. The results can be applied for optimizing a suitable extended-range microspeaker system.

Keywords: A suitable extended-range microspeaker system, Mirospeaker, Mobile device, Bass extension.

1. INTRODUCTION

Miniaturization with best-in-class audio performance is the trend for portable consumer electronics (3C) devices, such as tablets, detachable devices, and convertible devices. The loudspeaker systems in such devices must play audio signals with an acceptable loudness and sound quality, and a current challenge is bass extension in thin devices. A woofer system is an implementation that enhances the bass performance as the "x.1" channel. The basic stereo system (2.0) consists of two channels of sound - left and right - produced by a pair of stereo speakers. Most speakers are powered by a receiver (or even a good amplifier), although more modern ones can bypass the need for such equipment through extra features and/or wireless connectivity. A 2.1 channel system is achieved as soon as you incorporate a separate subwoofer (the .1 part of surround sound) along with the stereo speakers. The benefits of choosing a 2.0 or 2.1 channel system are affordable simplicity. You can enjoy excellent audio for music, movies, and TV without the clutter of additional speakers and the wires that tend to come with. This paper explains a bass extension method.

In 1930, Thuras [1] patented a vented loudspeaker enclosure and described the principle of its operation. He thus explained the foundations for the modern knowledge of loudspeaker systems. In subsequent years, various authors [2-4, 6, 7-15] have described the theoretical basis of and practical solutions for selected loudspeaker systems, namely infinite-baffle, closed-box, vented-box, passive-radiator, multispeaker, and open-box systems.

The first bandpass loudspeaker system was presented in a patent by D'Alton [16]. He described a sixth-order asymmetrical system. However, this system is not the subject of the patent: the inventor cited it as a "known form of a loudspeaker system." Lang [17] patented the first fourth-order bandpass loudspeaker system. His patent includes simple rules for system design. Thus far, the bandpass loudspeaker system has the most favorable low-frequency properties because of a compromise among efficiency, bandwidth, enclosure size, and diaphragm displacement. This speaker's advantages include high-quality sound reproduction in the low frequency range, small dimensions, low nonlinear distortion, and the ability to be placed anywhere in a room or car. Bandpass loudspeaker systems are used widely

* Corresponding author (Jackie.chang@acer.com)

DOI : 10.1017/jmech.2018.28
Copyright © 2018 The Society of Theoretical and Applied Mechanics
https://doi.org/10.1017/jmech.2018.28 Published online by Cambridge University Press

as subwoofers in home theaters and to provide sound in any venue, including cinemas, theaters, concerts, discotheques, opera houses, concert halls, and open-air amphitheaters. Various designs are mass-produced by manufacturers. Bandpass loudspeaker systems were investigated by Fincham [18] in 1979, Geddes [19] in 1989, Backman [20] in 1992, and Berkhoff [21] in 1994.

The common solution for bass extension is designing a woofer system for installation in mobile devices. However, currently available transducers can approach 250Hz of resonance frequency in free air for the minimal size of a speaker is ϕ25 mm × 9 mm, the speaker performance can be a woofer application; thus, the size of speakers cannot fit inside a mobile device, such as 10 inch tablet or ultra-thin laptop. This paper presents a solution to this problem that involves using a resonant combination of a front chamber and a rectangular, long, pipe-shaped port in front of speaker diaphragm. The efficient resonant coupling of the microspeaker system to the acoustic load in this structure enables a microspeaker with modest cone displacement to achieve a high sound pressure level (SPL) and bass extension below the resonance of the microspeaker in free air; additionally, the total dimensions of the structure are minimized. This solution was implemented in a 10 inch tablet (267.4 mm [L] × 169.2 mm [W] × 8.95 mm [H]) to achieve high bass extension performance. The results indicate that the design exhibits high bass extension performance and the SPL is enhanced in the bass response region.

2. METHODS OF SOLUTION

In the proposed design for bass extension employs the most frequently used rectangular microspeaker (9 mm × 16 mm × 2.5 mm) with five magnets. The dimensions of the microspeaker make it easy to install inside a mobile device. A cross-sectional sketch of a typical direct-radiator microspeaker is shown in Fig. 1. The diaphragm is suspended by a cone, and it is composed of polyetheretherkerketone with aluminum, which is supported at the outer edge and near the voice coil to ensure that it can move only in an axial direction.

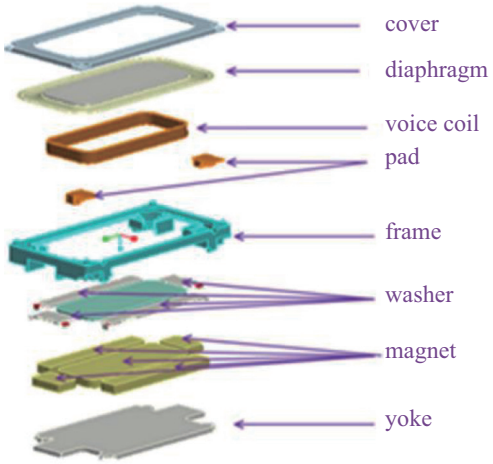


Fig. 1 Exploded view of a rectangular microspeaker (9 mm [W] × 16 mm [L] × 2.5 mm [H]).

2.1 Resonant Acoustic Enclosure of Microspeaker System

The proposed solution uses a resonant combination of a front chamber and a rectangular, long, pipe-shaped port. Our focus is propagation in rectilinear and uniform pipes or acoustic pipes with a constant cross section. We consider rectangular pipes with ideally rigid and smooth walls, filled with a compressible fluid, such as air, without losses. Consider a pipe with a rectangular cross section, sides l_y and l_z, and length l_x, where $l_x >> l_y > l_z$: it is a long, thin rectangular enclosure in which the modes (m_x, 0, 0) are plane waves along the x-axis. With these proportions for the pipe, and when the system is in a steady state at a frequency f below the frequency f_{010} of the mode (0, 1, 0), that is, $f < c/2l_y$, we have only plane waves, as only the axial modes (m_x, 0, 0) contribute to the sound field. A pipe is in a plane mode when only plane waves travel along its axis. For a rectangular pipe with a large side a, this is the case if $ka < \pi$ or $a < \lambda/2$. From a practical perspective, the most crucial quantities are the SPL and particle velocity. For a plane wave along the x-axis, we have

$$P(x)(P_a) = P_+(x) + P_-(x) = P_{+o}\exp(-jkx) + P_{-o}\exp(+jkx) \quad (1)$$

$$v(x)(m/s) = v_+(x) + v_-(x) = v_{+o}\exp(-jkx) + v_{-o}\exp(+jkx) \quad (2)$$

To solve a problem involving plane waves, we must determine the values of P_{+o}, P_{-o}, v_{+o}, and v_{-o}. We already have the following two relations:

$$P_{+o}(Pa) = Z_c v_{+o} \quad (3)$$

$$P_{-o}(Pa) = -Z_c v_{-o} \quad (4)$$

Z_c is the characteristic acoustic impedance of the medium. When the system is in a sinusoidal state, which means diaphragm of microspeaker is operated in piston behavior without higher order deformation, the relations in Eqs. (1)-(4) enable the determination of the sound field in a pipe from the boundary conditions, that is, at both ends of the pipe, at x = *0* and x = *l*.

Because the acoustic quantities, particularly the particle velocity $\underline{v}(x)$, are constant for the cross section S of the pipe, the particle velocity is substituted for the volume velocity q, as described previously [22] for sources:

$$q(x)(m^3/s) = S\underline{v}(x) \quad (5)$$

The relations in Eqs. (3) and (4) become

$$P_{\pm}(Pa) = \pm Z_{ac} q_{\pm} \quad (6)$$

where $Z_{ac} = Z_c/S$ (Ω_a). More generally, an acoustic impedance $Z_a(x)$ is introduced, and the radiation impedance is already defined [23].

$$Z_a(x)(\Omega_a) = p(x)/q(x) \quad (7)$$

The simple concept of the solution is shown schemat-

https://doi.org/10.1017/jmech.2018.28 Published online by Cambridge University Press



Fig. 2 Simple concept of the solution.

ically in Fig. 2. A relatively long rectangular pipe is in front of a chamber with a small volume. Here, *VR* is the rear chamber volume, and *VF* is the front chamber volume. *Sp* is the cross section of the pipe, and *Lp* is the length of the pipe.

In a steady state, a sound source is placed at the entrance of the pipe ($x = 0$), and an acoustic load is placed on the other extremity ($x = l$). The source is represented by an oscillating piston of volume velocity q_o, assumed to have an area equal to that of the cross section S of the pipe. According to the fundamental radiation hypothesis [24], with the particle velocity being normal and uniform on the piston, we have

$$q_o(m^3/s) = q_{+o} + q_{-o} \tag{8}$$

When the entrance of the pipe is subjected to an incident sound field, we consider a fictitious piston of a volume velocity such that at $x = 0$, the total external sound pressure (p_e) is equal to that at the entrance of the pipe (p_o). The pipe can be ended by perpendicular termination of any material. The input impedance is the value Z_a at $x = 0$, denoted Z_{ao}, and depends on the load impedance defined [25].

$$Z_{ao}(\Omega_u) = Z_{ac}[Z_{al} + jZ_{ac}\tan(kl)]/[Z_{ac} + jZ_{al}\tan(kl)] \tag{9}$$

Consider an oscillating piston of volume velocity q_o at $x = 0$. It is subjected to a sound pressure $Z_{ao} \cdot q_o$ and therefore to a force

$$F_o(N) = S^2 Z_{ao} v = Z_{mo} v \tag{10}$$

where v is the velocity and Z_{mo} is the mechanical impedance representing the reaction of the pipe on the piston.

The concept of Fig. 2 is a pipe with an open end. By assuming $ka < 1$, we neglect the radiation impedance. The boundary condition at $x = l$ is zero on the basis of Eq. (1), and according to Eq. (8), at $x = 0$, we easily determine the following Eqs (11) and (12)

$$q(x)(m^3/s) = q_o \cos k(1-x)/\cos kl \tag{11}$$

$$p(x)(Pa) = jZ_{ac} q_o \sin k(l-x)/\cos kl \tag{12}$$

The input impedance is

$$Z_{ao}(\Omega_u) = jZ_{ac}\tan kl \tag{13}$$

The resonances for $kl = (2n + 1)\pi/2$, $f_p = (2n + 1)c/4l$, c is the speed of sound (343 m/s), and $n = 0, 1, \cdots$, when l is an odd integer multiple of a quarter of the wavelength ($\lambda/4$), f_p is the natural frequency of the concept design.

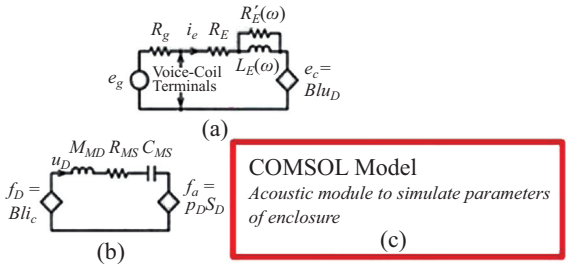


Fig. 3 Hybrid model.

2.2 Lumped and Finite Element Analyses of Microspeaker with Enclosure Design Parameters

Part of the Electo-Mechanic-Acoustic analogous circuit was used to model the microspeaker system in COMSOL Multiphysics software, in which all the variables of the electrical, mechanical, and acoustical domains can be analyzed with a unified framework. According to the preceding theory, the methodology of acoustic module and speaker models was employed by Chang and Wang [26], the methodology presented to predict the microspeaker system frequency response with the enclosure parameters, as illustrated by the schematic in Fig. 3. The acoustic module of the COMSOL Multiphysics software is employed instead of an acoustic circuit in the acoustical domain by using the finite element method.

The dynamics of each subsystem are lumped into a single impedance element. The coupling of the electrical and mechanical domains is modeled by a gyrator, with the mechanical system represented by the impedance analogy, whereas the coupling of the mechanical and acoustical domains is modeled by a transformer. The impedance of the acoustical system is discussed in detail to demonstrate our differentiation model. The steady-state and transient responses can be predicted readily with the aid of equivalent circuits. The electrical system consists mainly of the voice coil and can be modeled as an inductor L_E and a resistor R_E whose electrical impedance is written as

$$Z_E = R_E + j\omega L_e \tag{14}$$

The mechanical system comprising the diaphragm, voice coil, and suspension is modeled as a second-order system with the following mechanical impedance:

$$Z_M = j\omega M_{ms} + R_{MS} + \frac{1}{j\omega C_{MS}} \tag{15}$$

The impedance of the acoustical system is more complex than those of the other two subsystems. This greater complexity is attributed to the effects of cavities, ducts, perforations, and radiation loading associated with the mobile enclosure. Here, it can be simplified by lumping the acoustical impedances together into two terms from the front (Z_{AF}) and back (Z_{AB}) of a microspeaker with a system enclosure,

$$Z_A = Z_{AF} + Z_{AB} \tag{16}$$

https://doi.org/10.1017/jmech.2018.28 Published online by Cambridge University Press

Table 1 Microspeaker parameters.

Electrical Parameters			1	2	3	4	5	AVG
R_e	Electrical voice coil resistance at DC	Ohm	7.08	7.1	7.12	7.13	7.12	7.11
L_e	Frequency independent part of voice coil inductance	mH	0.034	0.033	0.033	0.033	0.033	0.0332
Mechanical Parameters								
M_{ms}	"Mechanical mass of driver diaphragm assembly including air load and voice coil"	g	0.06	0.063	0.064	0.062	0.062	0.0622
R_{ms}	Mechanical resistance of total-driver losses	kg/s	0.106	0.117	0.117	0.119	0.108	0.1134
C_{ms}	Mechanical compliance of driver suspension	mm/N	1.001	0.911	0.879	0.937	0.946	0.9348
K_{ms}	Mechanical stiffness of driver suspension	N/mm	1	1.1	1.14	1.07	1.06	1.074
Bl	Force factor (Bl product)	N/A	0.769	0.773	0.792	0.769	0.776	0.7758
Other Parameters								
V_{as}	Equivalent air volume of suspension	1	0.0011	0.001	0.001	0.0011	0.0011	0.00106
S_d	Diaphragm area	cm^2	0.9	0.9	0.9	0.9	0.9	0.9

The coupling of the electrical and mechanical domains is represented by a gyrator that follows two electrodynamical laws,

$$f = Bli \tag{17}$$

$$e = Blu \tag{18}$$

where i is the current flowing in the voice coil, e is the voltage induced by coil motion across the voice-coil terminals, f is the Lorentz force produced by the current, and u is the cone velocity of the diaphragm. Two basic variables in the acoustical domain are the pressure P and volume velocity q. The coupling of the mechanical and acoustical domains can be simulated by a transformer, according to the following relations between P and q_o:

$$f = S_D P \tag{19}$$

$$q_o = S_D u(x) \tag{20}$$

The volume velocity q_o emitted by a source is the time derivative of the volume of air it displaces. Consider a microspeaker mounted in a closed box with the parameters in Table 1. Let S_D, X_D, and q_o denote the diaphragm piston area, displacement, and velocity, respectively. The volume of air displaced is $V = S_D x$. The volume velocity emitted is expressed in Eq. (20). The equivalent piston area of a diaphragm is defined as the area of a flat piston that emits the same volume velocity. The rule states that the piston radius in centimeters is equal to the documented diameter. The phase volume velocity emitted is given by

$$U = 4\pi r^2 u_r(r) = 4\pi r^2 \frac{P(r)}{Z_s} = \frac{4\pi K}{j\omega\rho}\left[1 + j\frac{\omega r}{c}\right]\exp(-jkr) \tag{21}$$

After the network has been solved for the required volume velocities, the far-field acoustic pressure P can be calculated by assuming that the system behaves as a point source.

$$P = j\frac{\rho c k}{2\pi r} U_t \exp j(\omega t - kr) \tag{22}$$

where ρ is the density of air, c is the velocity of sound in air, ω is the angular frequency ($\omega = kc$), k is the wavenumber ($k = 2\pi/\lambda$), U_t is expressed in Eqs. (11) and (21), and r is the distance from the source to the observation point. The on-axis pressure radiated is defined by Eq. (22). The SPL is defined by

$$SPL = 20\log\left(\frac{P}{P_{ref}}\right) \tag{23}$$

where $P_{ref} = 2 \times 10^{-5}$ Pa.

Before implementing the simulation, we investigated the lumped parameters of the microspeaker through a Klippel system to acquire the Thiele-Small (TS) parameters under a small signal with a Vrms of 0.1 V. To ensure the accuracy of the TS parameters (Table 1), we evaluated five samples and averaged the results. The parameters were set in our model to produce a uniform positon velocity; the acoustic domain of the microspeaker and the enclosure parameters were simulated using the COMSOL finite element model.

To measure the sound pressure response of the microspeaker system in an anechoic chamber, the B&K PULSE Electroacoustics system in addition to sound check software and a highly sensitive microphone (B&K Type 4191) were used. The frequency range of the microspeaker from 100 to 20 KHz was measured using a 1 W sweep sine input. A schematic of the experimental apparatus is shown in Fig. 4 and presents the experi-

https://doi.org/10.1017/jmech.2018.28 Published online by Cambridge University Press

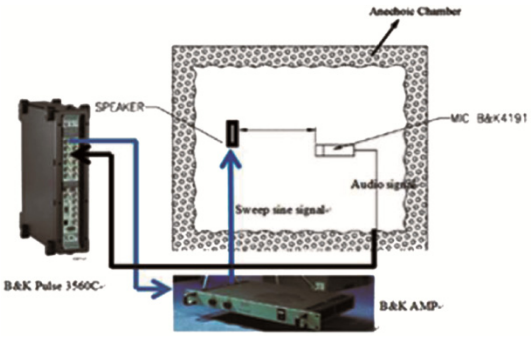


Fig. 4 Measurement setup.

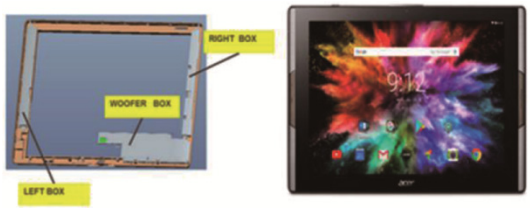


Fig. 5 10 inch tablet (267.4 mm [L] × 169.2 mm [W] × 8.95 mm [H]).

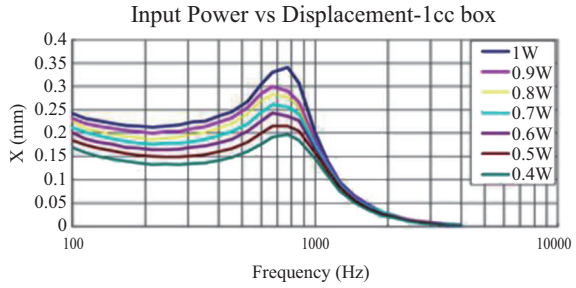


Fig. 6 Input Power vs diaphragm displacement.

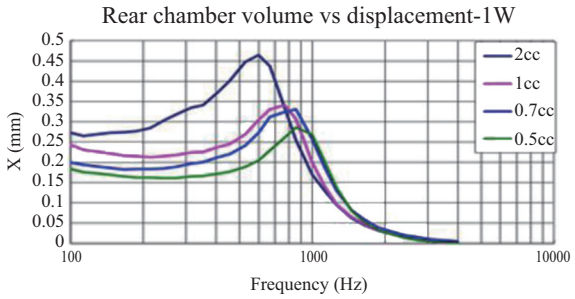


Fig. 7 Rear chamber volume vs diaphragm displacement.

Table 2 Design parameters for bass extension of a microspeaker system.

Version	V0322	V0328
Total volume	4.7 cc	3.93 cc
Speaker driver	16 mm × 9 mm × 2.5 mm	16 mm × 9 mm × 2.5 mm
Opening area (mm^2)	35.7 mm^2	45.7 mm^2
Front chamber size(cc)	0.18 cc	0.13 cc
Rear chamber size (cc)	1 cc	1 cc
Channel length (mm)	291.65 mm	188.23 mm
Section area of channel (mm^2)	13 mm^2	19.5 mm^2
Equivalent volume of channel (cc)	3.53 cc	2.8 cc

mental arrangement for measuring the on-axis SPL response by using a microphone positioned 50 cm from the microspeaker system.

3. RESULTS

Lack of bass response is always a problem in mobile devices, and the trend for the form factor is "as thin as possible" in the current consumer market. The designed microspeaker system was implemented in a 10 inch tablet (267.4 mm [L] × 169.2 mm [W] × 8.95 mm [H]) (Fig. 5). The tablet's original design has left and right channel speaker modules, but the bass response is insufficient. When microspeaker of 9 mm × 16 mm × 2.5 mm was designed, its rear chamber volume is only close to 1cc, the system resonance of the speaker module is only close to 900 Hz. Although the large back chamber has high compliance and the box resonance frequency is low, we observed some hardware limitations regarding power handling and diaphragm displacement.

We used a 1 cc rear chamber volume to study input power level versus diaphragm displacement (Fig. 6). Experimental results showed that the diaphragm displacement is proportional to the input power level. Loudspeaker diaphragm displacement is well known to be proportional to drive voltage and thus proportional to the square root of the input power. Consider this, Fig. 6 shows a displacement of 0.17 mm for 0.4 W input power and a displacement of 0.23 mm for 0.8 W input power. We also studied the relationship between the rear chamber volume and diaphragm displacement (Fig. 7). The results showed that if the rear chamber volume is large, diaphragm displacement is excessive and mechanical damage is expected. Based on these results, increasing the rear chamber volume for bass extension is not recommended.

As mentioned in section 2.1 and section 2.2, we designed two microspeaker systems to enhance the bass extension. The design parameters are presented in Table 2.

https://doi.org/10.1017/jmech.2018.28 Published online by Cambridge University Press

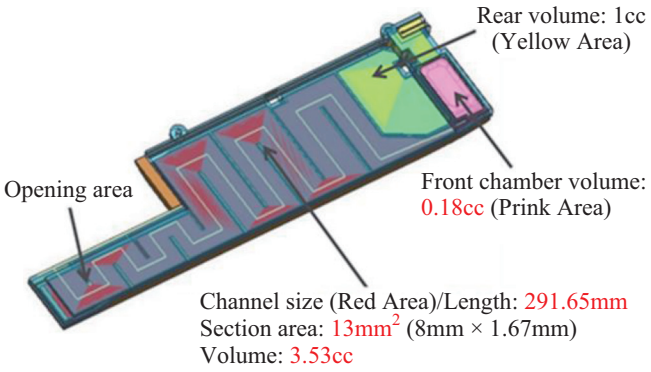


Fig. 8 Initial design (V0322).

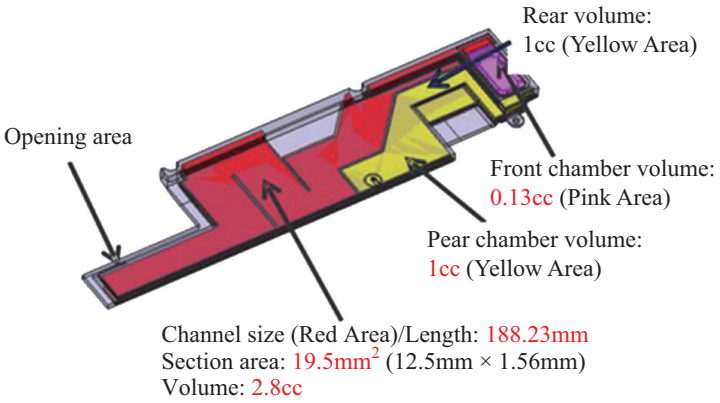


Fig. 9 Simulation and measurement of final design (V0328).

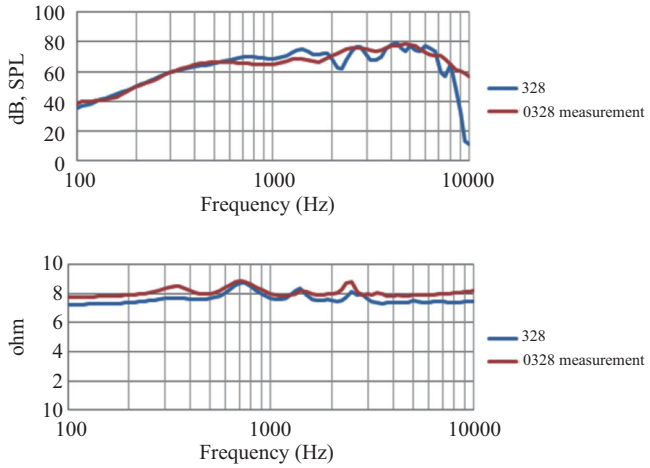


Fig. 10 Simulation and measurement of final design (V0328).

The solution with an optimal rear chamber volume of 1 cc and a resonant combination of a coupling front chamber and a rectangular, long, pipe-shaped port was studied. Our solution can resolve diaphragm displacement attributable to high power handling and a large rear chamber volume. The first prototype is presented in Fig. 8, and the final prototype is presented in Fig. 9. Both the first and final prototypes have a rear chamber volume of 1 cc to prevent the mechanical damage caused by large diaphragm displacement and to optimize the power handling and thus attain a high SPL. The 9 mm × 16 mm × 2.5 mm microspeaker was placed on a flat surface, and we set a small front chamber volume (0.1 cc~0.2 cc) to propagate the sound to the long rectangular pipe; the prototype is similar to a closed-open type. The plane wave can excite the natural frequencies and modes of a long pipe-shaped port.

In Fig. 10, the simulation results of frequency re-

https://doi.org/10.1017/jmech.2018.28 Published online by Cambridge University Press

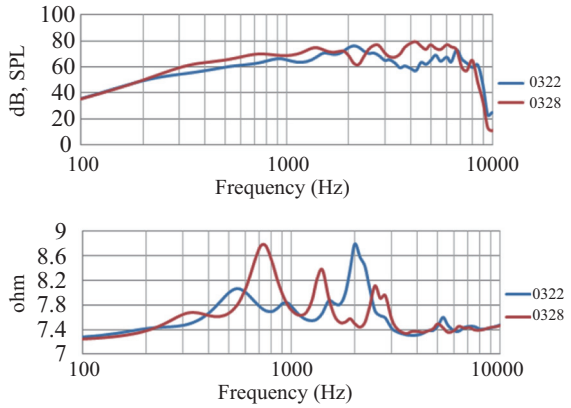


Fig. 11 Comparison results of V0322 and V0328.

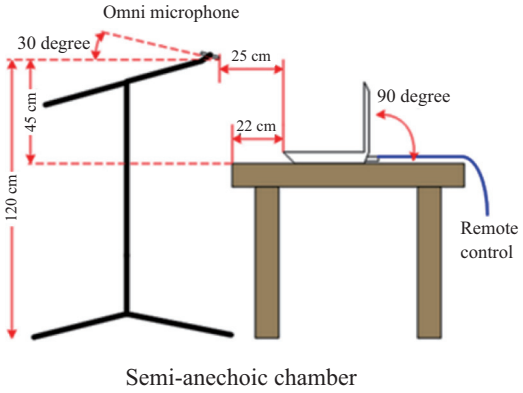


Fig. 12 System measurement setup.

sponse and impedance curve are in agreement with the experimental results, which are based on our final prototype design (In Fig. 9). In Fig. 11, the first resonance frequency of the first prototype (V0322) is lower than 300 Hz and the first resonance frequency of the final prototype (V0328) is lower than 400 Hz. Both are lower than the resonance frequency of the microspeaker in free air (fo = 450 Hz). The solution to extend the bass performance is successful. The results of the comparison of the first and final prototypes' audio performance according to the SPL and bass response are also presented in Fig. 11. Although the first prototype has lower bass extension, but its sensitivity is lower than that of the final prototype by at least 6 dB, SPL increases as the channel area increases; therefore, we implemented the final prototype in the 10 inch tablet (Fig. 5).

The system measurement setup, designed in consideration of user behavior, is shown in Fig. 12. A semi-acoustic chamber or anechoic chamber can be used to evaluate system audio performance. Wideband pink noise of −6 dBFS was installed on the tablet, and a media player was used to broadcast the test source through a software decoder, postprocessing unit, and speaker amplifier to drive the left and right channel speaker modules and the thin woofer system. Among two similar devices, one has stereo speaker system with an integrated thin woofer system—called "Titan" and

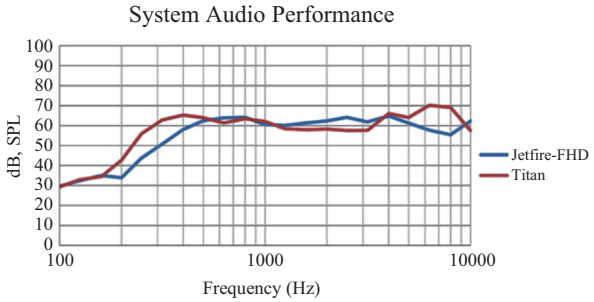


Fig. 13 Audio performance of final system.

one without, the Titan has the bass response ranged from 200 to 500 Hz (Fig. 13). Titan exhibited improvement by approximately 10 dB, and bass extension was well implemented. In Fig. 13, the bass range is from 200 Hz to 500 Hz, it is contributed by a suitable extended-range microspeaker system of final prototype design, the mid and high frequency response are controlled by left channel speaker and right channel speaker with high-pass effect. Thus, the optimal suitable extended-range microspeaker system based on a microspeaker inside a thin tablet was successfully applied. The benefit of this implementation on tablet can well perform upper bass band (160~300 Hz, warmth, or a muddy, woody sound. fundamental for snare, toms, guitars, male vox) and low-mid (300~800 Hz, this range has lots of upper resonance & droning.).

4. DISCUSSION

Different form factors are associated with different microspeaker system performance levels, rendering prediction of the final performance challenging. As mentioned, the SPL response and bass performance are the coupled output of various parameters. Each design parameter has a unique implication for the SPL response and bass performance. The theoretical comparison of the lumped model with the distribution model of enclosure parameters, as previously described, was conducted to achieve an SPL simulation in agreement with the experiment conducted in the low- and high-frequency ranges of sounds audible to human ears. The final prototype (V0328) served as the basis for the subsequent parametric experiments. We focused on qualitative and quantitative research of the output SPL and bass response of five design cases (Table 3).

4.1 Case A, front Chamber Opening Area

The front chamber opening area affects the SPL response of complete microspeaker driver units. We investigated two cases of the front chamber opening area, with the back chamber volume maintained at 1 cc (Table 3), by using the final prototype (V0328) [Figs. 14 (a) and (b)]. Figure 14 (a) depicts the unit with the original front chamber opening area (45.7 mm^2), and Fig. 14 (b) depicts the unit with a front chamber opening area 1.5

https://doi.org/10.1017/jmech.2018.28 Published online by Cambridge University Press

Table 3 Design parameters of a suitable extended-range microspeaker system based on the microspeaker.

Case	Item	Parameters	Reference Picture
A	Front opening area effect	Parameters: 45.7 mm^2 × 1, 45.7 mm^2 × 1.5 Fixed condition: Front opening area of 45.7 mm^2 (1 cc for rear volume, 0.13 cc for front chamber volume, channel length is 188.82 mm and cross section area is 19.5 mm^2)	Fig 14 (a)-case 1, (b)-case 2
B	Front chamber volume	Parameters: 0.5cc, 1cc. Fixed condition: Front opening area of 45.7 mm^2 (1 cc for rear volume, 0.13 cc for front chamber volume, channel length is 188.82 mm and cross section area is 19.5 mm^2)	Fig. 14 (c)-case 3, (d)-case 4
C	Rear chamber volume	Parameters: 0.5cc, 1.5cc. Fixed condition: Front opening area of 45.7 mm^2 (0.13 cc for front chamber volume, channel length is 188.82 mm and cross section area is 19.5 mm^2)	Fig 14 (e)-case 5, (f)-case 6
D	Channel length	Parameters: (188.2 mm) × 0.5; (188.2 mm) × 1.5; (188.2 mm) × 2 Fixed condition: Front opening area of 45.7 mm^2 (1 cc for rear volume, 0.13 cc for front chamber volume and cross section area is 19.5 mm^2)	Fig. 14 (g)-case 7, (h)-case 8, (i)-case 9
E	Cross section of internal channel	Parameters: (19.5 mm^2) × 0.5; (19.5 mm^2) × 1.5; (19.5 mm^2) × 2 Fixed condition: Front opening area of 45.7 mm^2 (1 cc for rear volume, 0.13 cc for front chamber volume, channel length is 188.82 mm)	Fig. 14 (j)-case 10, (k)-case 11, (l)-case 12

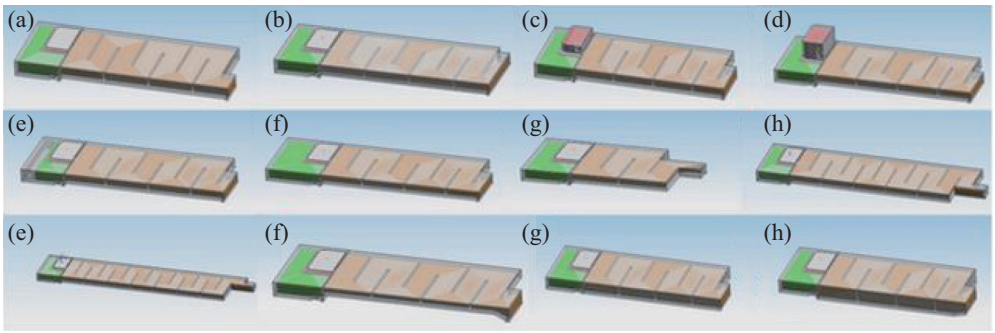


Fig. 14 Schematics of cases 1-12.

times that of the original. We examined the two cases to explain their effects on the SPL curve and cutoff frequency of the low-pass filter.

For the cases considered, the SPL curves were obtained using lumped and finite element models as well as experiments. The measurement results and simulated SPL curves derived for the two cases are presented in Figs. 15 (a) and (b), respectively. Comparing the simulated SPL curves and measurement results reveals that both curves exhibit a consistent trend; specifically, increasing the area (open rate) of the front chamber opening port can facilitate a reduction of the rise-up effect of f_h (resonance at high frequency) and enhance the SPL by 10 dB above 7500 Hz. The results demonstrate that the original chamber opening area is sufficient to yield an SPL response higher than that of the final prototype (V0328) by approximately 10 dB at 1 KHz, and the high-frequency response is extended beyond 10 KHz.

4.2 Case B, front Chamber Volume

The case involving the 1 cc back chamber volume shows that if an industrial design provides a 45.7 mm^2 opening area for the sound port to reduce radiation impedance, then the placement of a microspeaker within the enclosure impairs the production of the front chamber. To investigate the effect of the front chamber volume, two volumes, namely, 0.5 and 1 cc, were considered. Based on the final prototype (V0328), schematics are presented in Figs. 14 (c) and (d).

The front chamber volume was determined to be a

https://doi.org/10.1017/jmech.2018.28 Published online by Cambridge University Press

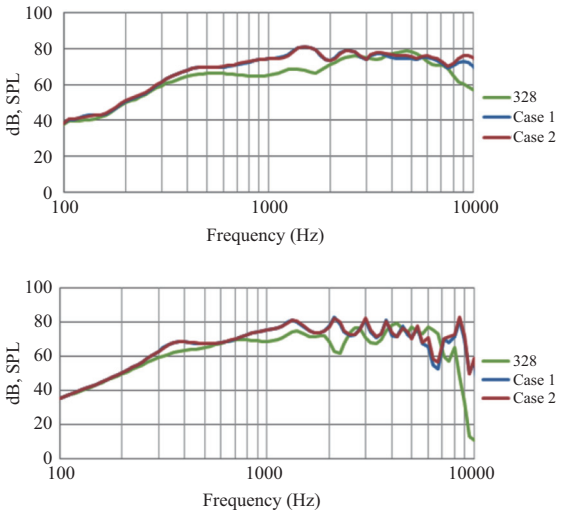


Fig. 15 V0328, cases 1 and 2: (a) measurement comparison; (b) simulation comparison.

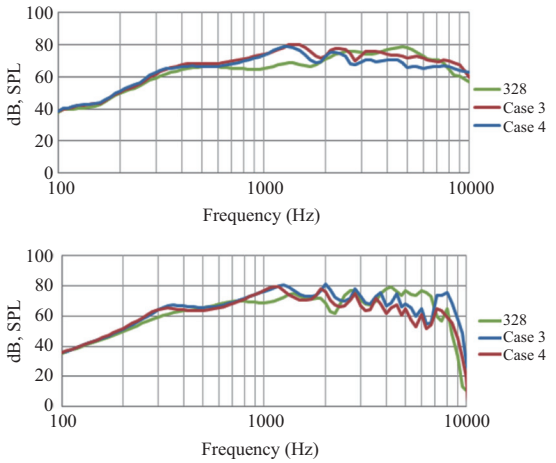


Fig. 16 V0328, cases 3 and 4: (a) measurement comparison; (b) simulation comparison.

critical factor affecting f_h. The cases of 0.5 cc [f_h = 3150 Hz] and 1 cc [f_h = 4500 Hz] are illustrated in Figs. 16 (a) and (b). From an SPL perspective, a front chamber volume of 0.5 cc is superior to that of the final prototype (V0328), which is only 0.13 cc because the thickness of the tablet is restricted. In the simulation, modifying the front chamber volume resulted in variations of the compliance and sound transmission. The simulated SPL curves derived for the two cases are plotted in Fig. 16 (b). The simulated results indicate that smaller front chamber volumes are preferable because broader smooth regions from 300 Hz to 10 KHz are produced. However, the front chamber volume between the microspeaker and port must have a minimal value for free vibration of the diaphragm.

A comparison of cases 1 and 2 revealed that if the front chamber volume is the same and the opening area is increased, the high-frequency response is extended. Based on that finding, a small front chamber volume and large opening area are optimal and do not affect the high-frequency response. The SPL improvement from 400 Hz to 2 KHz is related to the optimal front chamber volume of 0.5 cc.

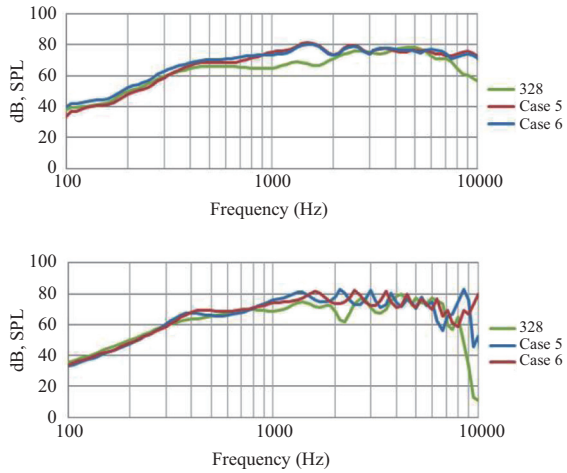


Fig. 17 V0328, cases 5 and 6: (a) measurement comparison; (b) simulation comparison.

4.3 Case C, Rear Chamber Volume

Generally, a microspeaker simultaneously produces sound from its front and back. The phases of both sound sources are opposite, and consequently, the interference between them leads to the degradation of the overall SPL and frequency response. For experiments in an anechoic chamber, installing a baffle enables data collection from the front source only. Specifically, sound interference from the back of the microspeaker is usually blocked by an enclosure or a baffle-like structure. To investigate the enclosure effect, three distinct back enclosure volumes, namely 0.5, 1.5, and 2 cc, were considered. Based on the final prototype (V0328), schematics are shown in Figs. 14 (e) and (f).

The enclosed air provides a compliance that also serves to limit the low frequency excursion of the driver unit, improving longevity. Notably, hermetically sealing the enclosure may be ill-advised because any changes in atmospheric pressure cause changes in the equilibrium position of the driver.

Figures 17 (a) and (b) illustrate the effect of the rear chamber volume, indicating that the box is large and the compliance of the enclosed air is high. The compliance of the driver unit is predominant, and the enclosure serves merely to isolate the rear radiation. However, in the acoustic suspension design, the enclosure is sufficiently small to exert a controlling influence on the effective compliance of the system. The front face of the driver is the only source of acoustic radiation. In this case, the large back chamber volume has high compliance, and the box resonance frequency is low. The rear chamber volume contributes an only 50 Hz extension to the bass range, and the SPL is approximately 5 dB higher than that of the final prototype (V0328) at 600 Hz. Bass extension is contributed by the resonance of the pipe-shaped port, not the rear chamber volume. To

https://doi.org/10.1017/jmech.2018.28 Published online by Cambridge University Press

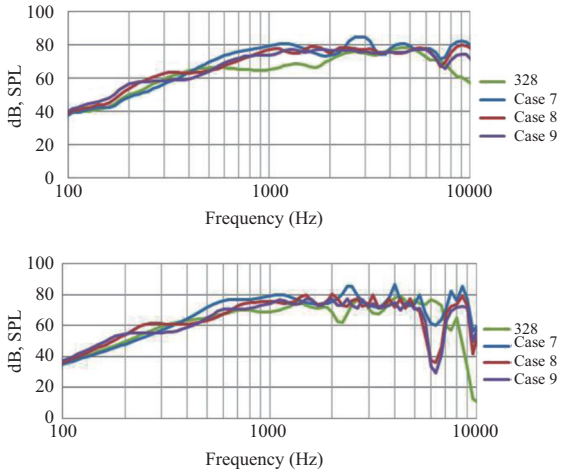


Fig. 18 V0328, cases 7, 8, and 9: (a) measurement comparison; (b) simulation comparison.

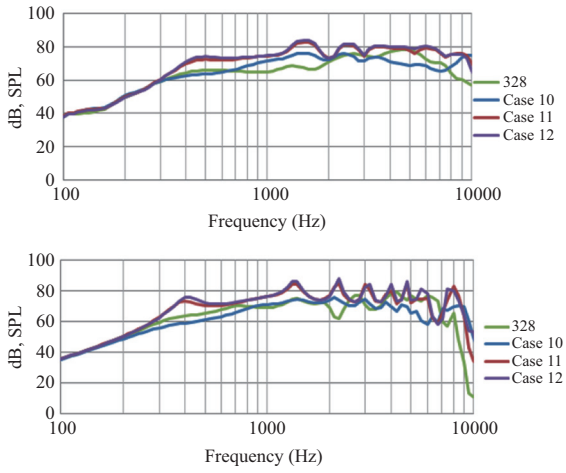


Fig. 19 V0328, cases 10, 11, and 12: (a) measurement comparison; (b) simulation comparison.

resolve the power handling problem and large diaphragm displacement, the optimal rear chamber volume must remain at 1 cc.

4.4 Case D, Channel Length

The case involving the 1 cc back chamber volume demonstrates that if an industrial design provides a 45.7 mm^2 opening area for the sound port to reduce radiation impedance, then the placement of a microspeaker within the enclosure impairs the production of a front chamber with a volume of 0.13 cc. To investigate the effect of the channel length, three channel lengths were considered: 188.2 mm × 0.5, 188.2 mm × 1.5, and 188.2 mm × 2. Schematics, based on the final prototype (V0328), are presented in Figs. 14 (g), (h), and (i).

As described in section 2.1 and section 2.2, the resonance of the pipe can be calculated and simulated. The front channel length was determined to be a critical factor affecting f_L. In case 7, where the length is 188.2 mm × 0.5, f_L is higher than the resonance of the microspeaker in free air; in case 8, where the length is 188.2 mm × 1.5, f_L = 300 Hz; and in case 9, where the length is 188.2 mm × 2, f_L = 200 Hz.

The simulation and measurement results revealed that modifying the front channel length resulted in variations of the pipe's resonance by exciting a plane wave of the microspeaker to transmit sound. The measurement results and simulated SPL curves derived for the three cases are plotted in Figs. 18 (a) and (b). The simulation results demonstrate that a long front channel length is preferable because broader smooth regions from 200 Hz to 10 KHz are produced. As illustrated by the simulation and measurement results of case 7, when the channel length is only half that of the final prototype design (V0328), the bass response is higher than that of the final prototype design (V0328) by approximately 300 Hz. For case 8, the simulated SPL curve and measurement results show bass extension to 250 Hz. For case 9, the simulated SPL curve and measurement results show bass extension to 200 Hz. However, the front channel length between the front chamber and the port must have an optimal value for the unit to fit inside a mobile device. A comparison of these cases with cases 3 and 4 demonstrates that an increase in the front channel length can contribute to greater bass extension than an increase in the rear chamber volume.

4.5 Case E, Cross-Sectional Area of Internal Channel

In practice, design constraints prevent most cross-sectional areas of an internal channel from being located at the center of the diaphragm. The simulation and measurement results show that the cross-sectional area of the internal channel in various locations can enhance the sound directivity in terms of the axial acoustic pressure. For case E, samples based on the final prototype (V0328) were prepared; schematics are presented in Figs. 14 (j), (k), and (*l*).

For the three cases, the SPL curves obtained through simulation and measurement are plotted in Figs. 19 (a) and (b). In Case 10, the cross-sectional area is half that of the original front channel; the SPL in the low-frequency range is lower than that of the original design (V0328), but the SPL is markedly improved between 1 and 2 KHz. For case 11 and case 12, the overall sensitivity is greater than that of the final prototype (V0328) by approximately 10 to 15 dB, but the bass response is not obviously shifted. The sensitivity seems to be proportional to the cross-sectional area of the internal channel.

5. CONCLUSIONS

A rigorous electroacoustic analysis, based on a lumped model and the finite element method, was conducted to investigate the influence of enclosure parameters on microspeaker driver units. The simulation results are in agreement with the experimental results. A resonant combination of a front chamber and a

https://doi.org/10.1017/jmech.2018.28 Published online by Cambridge University Press

Table 4 Conclusions regarding enclosure design parameters.

	Enclosure Design Parameter	Parameters	Influence of System Performance
Opening area effect	Sound hole of speaker module	45.7 mm^2 × 1	Bass cannot be extended, but the overall sensitivity can be increased and it is proportional to opening area. 10 dB up at 1 KHz area.
		45.7 mm^2 × 1.5	Bass cannot be extended, but the overall sensitivity can be increased and it is proportional to opening area. 10 dB up at 1 KHz area, SPL is higher than one time of opening area in 10 KHz.
Front chamber volume	Front open rate (1 cc rear volume)	0.5 cc, 1 cc	Bass cannot be extended, but f_H is shifted to low frequency area. Sensitivity is attenuated at high frequency. If front chamber volume is 1cc, f_H is lower than 0.5 cc of front chamber volume.
Rear chamber volume	Front chamber volume is 0.13 cc and opening area is 45.7 mm^2	0.5 cc, 1.5 cc	Bass cannot be extended. If rear chamber volume is large, the overall sensitivity will be increased.
Channel length	Front chamber volume is 0.13 cc, opening area is 45.7 mm^2 and rear chamber volume is 1 cc.	(188.2 mm) × 0.5 (188.2 mm) × 1.5 (188.2 mm) × 2	Bass can be extended to low frequency area and f_L (bass) is proportional to channel length.
Cross section area of channel	open hole location (1 cc rear volume, 50% open rate)	(19.5 mm^2) × 0.5 (19.5 mm^2) × 1.5 (19.5 mm^2) × 2	The f_L (bass) is not impacted, but the SPL can be enhanced. SPL is proportional to section area of channel.

rectangular, long, pipe-shaped port enables bass extension of a microspeaker system in a 10 inch tablet; the system achieves resonance below that of the microspeaker in free air. The efficient resonant coupling of the microspeaker system to the acoustic load in this structure enables a microspeaker with modest cone displacement to achieve a high SPL and bass extension; additionally, the total dimensions of the structure are minimized. When a thin woofer system based on a microspeaker was implemented in a 10 inch tablet, the SPL was improved by more than 10 dB from 200 to 500 Hz. Special attention was paid to the modeling of microspeaker enclosures; specifically, 12 cases were studied. The findings are summarized in Table 4 to provide a reference regarding bass extension design parameters. By investigating each of these parameters, engineers in the 3C industry can optimize the SPL performance and frequency bandwidth of their basic microspeaker design concepts to acquire a suitable extended-range microspeaker system before executing designs.

ACKNOWLEDGMENTS

The authors thank the National Science Council of the Republic of China, Taiwan, for financially supporting this research under Contract No. NSC 101-2221-E-002-102.

REFERENCES

1. Thuras, A. L., "Sound Translating Device," U.S. patent 1,869,178 (filed 1930; awarded 1932).
2. de Boer, E., "Synthesis of Bass-Reflex Loudspeaker Enclosures," *The Journal of the Acoustical Society of America*, **31**, pp. 246 (1959).
3. Thiele, A., "Loudspeakers in Vented Boxes," *Journal of the Audio Engineering Society*, **19**, pp. 382-392 (1971).
4. Benson, J. E., "Theory and Design of Loudspeaker Enclosures, Part 1: Electroacoustical Relations and Generalised Analysis," *Amalgamated Wireless Australasia Technical Review*, **14**, pp. 1-58 (1968).
5. Benson, J. E., "Theory and Design of Loudspeaker Enclosures, Part 2: Response Relationships for Infinite Baffle and Closed Box Systems," *Amalgamated Wireless Australasia Technical Review,* **14**, pp. 225-293 (1971).
6. Benson, J. E., "Theory and Design of Loudspeaker Enclosures, Part 3: Introduction to Synthesis of Vented Systems," *Amalgamated Wireless Australasia Technical Review*, **14**, pp. 369-484 (1972).
7. Small, R. H., "Direct-Radiator Loudspeaker Systems Analysis," *IEEE Transactions on Audio and Electroacoustics*, **19**, pp. 269-281 (1971).
8. Small, R. H., "Closed-Box Loudspeaker Systems, Part 1: Analysis," *Journal of the Audio Engineering Society*, **20**, pp. 798-808 (1972).
9. Small, R. H., "Closed-Box Loudspeaker Systems, Part 2: Synthesis," *Journal of the Audio Engineering Society*, **21**, pp. 11-18 (1973).
10. Small, R. H., "Vented-Box Loudspeaker Systems, Part 1: Small-Signal Analysis," *Journal of the Audio Engineering Society*, **21**, pp. 363-372 (1973).
11. Small, R. H., "Vented-Box Loudspeaker Systems, Part 2: Large-Signal Analysis," *Journal of the Audio Engineering Society*, **21**, pp. 438-444 (1973).

https://doi.org/10.1017/jmech.2018.28 Published online by Cambridge University Press

12. Small, R. H., "Vented-Box Loudspeaker Systems, Part 3: Synthesis," *Journal of the Audio Engineering Society*, **21**, pp. 549-554 (1973).
13. Small, R. H., "Vented-Box Loudspeaker Systems, Part 4: Appendices," *Journal of the Audio Engineering Society*, **21**, pp. 635-639 (1973).
14. Small, R. H., "Passive-Radiator Loudspeaker Systems, Part 1: Analysis," *Journal of the Audio Engineering Society*, **22**, pp. 592-601 (1974).
15. Small, R. H., "Passive-Radiator Loudspeaker Systems, Part 2: Synthesis," *Journal of the Audio Engineering Society*, **22**, pp. 683-689 (1974).
16. D'Alton, A., "Acoustic Device," U.S. patent 1,969,704 (filed 1933; awarded 1934).
17. Lang, H. C., "Sound Reproducing System," U.S. patent 2,689,016 (filed 1953; awarded 1954).
18. Fincham, L. R., "A Bandpass Loudspeaker Enclosure," Presented at the 63rd Convention of the Audio Engineering Society, *Journal of the Audio Engineering Society*, **27**, p. 600 (1979).
19. Geddes, E. R., "An Introduction to Band-Pass Loudspeaker Systems," *Journal of the Audio Engineering Society*, **37**, pp. 308-342 (1989).
20. Backman, J., "A Computational Model of Transmission Line Loudspeakers," Presented at the 92nd Convention of the Audio Engineering Society, *Journal of the Audio Engineering Society*, **40**, p. 438 (1992).
21. Berkhoff, A. P., "Impedance Analysis of Subwoofer Systems," *Journal of the Audio Engineering Society*, **42**, pp. 4-14 (1994).
22. Fahy, F., *Foundations of Engineering Acoustic*, Academic Press (2001).
23. Beranek, L. L., *Acoustics*, Acoustical Society of America, Woodybury, NY (1996).
24. Colloms, M., *High Performance Loudspeakers*, 5th Edition, John Wiley & Sons, NY (1997).
25. Kinsler, L. E., Frey, A. R., Coppens, A. B. and Sanders, J. V., *Fundamentals of Acoustics*, 4th Edition, John Wiley & Sons, NY (2000).
26. Chang, J. R. and Wang, C. N., "Acoustical Analysis of Enclosure Design Parameters for Microspeaker System," *Journal of Mechanics*, DOI:10.1017/jmech.2017.64 (2017).

(Manuscript received February 26, 2018,
accepted for publication May 17, 2018.)

https://doi.org/10.1017/jmech.2018.28 Published online by Cambridge University Press